Supporting Information

Formation of Gas-phase Hydrogen Peroxide via Multiphase Ozonolysis of Unsaturated Lipids

Zilin Zhou* and Jonathan P. D. Abbatt

Department of Chemistry, University of Toronto, 80 St. George Street, Toronto, ON, Canada M5S 3H6

*Corresponding author. Email: zilin.zhou@utoronto.ca

Table of Contents

1) Lipid structures

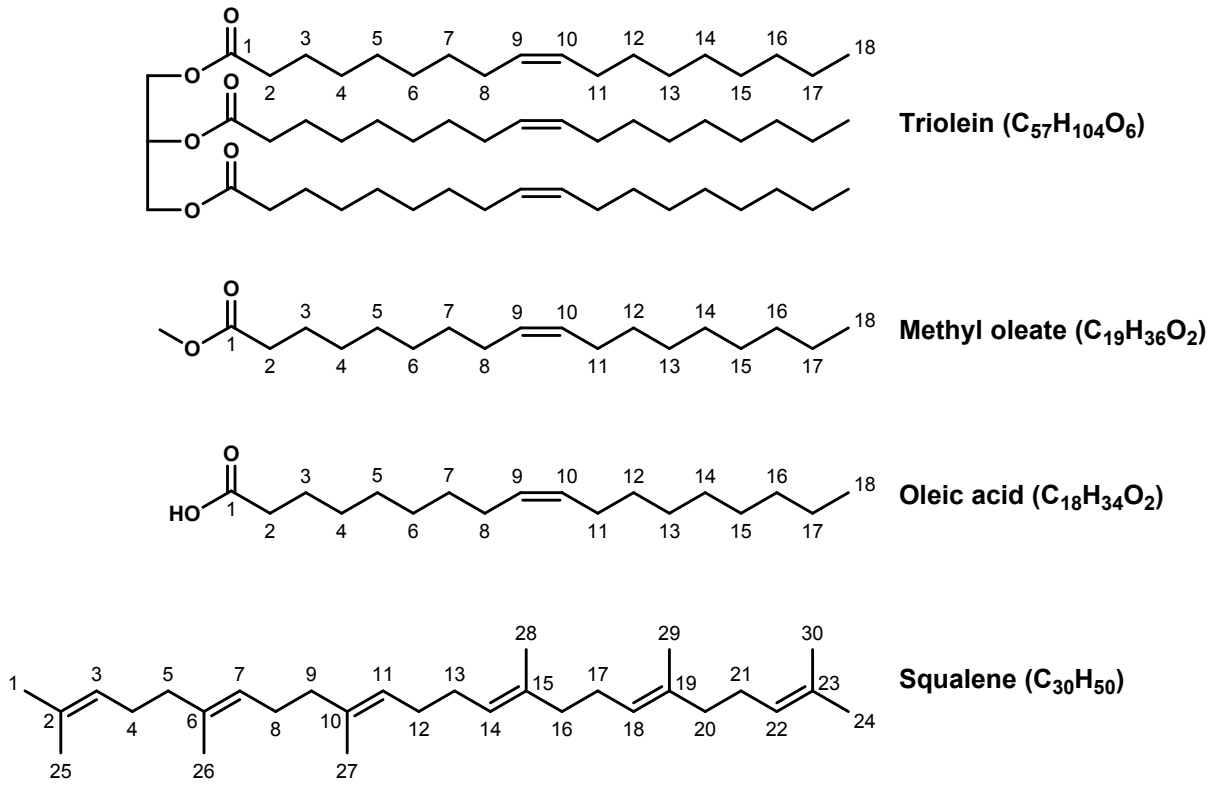

Figure S1: Chemical structures of pure lipids in this study.

2) Measurements and quantitation methods

In this study, ozone was sampled by an ozone monitor (2B Technologies model 202) every 10 s, while H_2O and H_2O_2 were measured simultaneously by an H_2O_2 analyzer (Picarro PI2114) every 3-4 s. According to instrument specifications, the detection limit of both analyzers is ≤3 ppb. The measured 1σ precision (10 minutes) was ≤10 ppb for 500 ppb ozone and ≤1 ppb for H_2O_2 in all experiments.

Prior to each experiment, the ozone loss caused by interactions with the reactor walls ($[O_3]_{wall}$) was determined by measuring the difference between ozone flowing through the bypass line and the reactor without lipids. The wall loss was typically < 5 ppb when 500 ppb ozone reactant air was applied. Note that the H_2O_2 loss on surfaces was considered negligible, according to a

previous study by Kahan et al.[1] As shown in Figure S2, each quantitation experiment consisted of four periods (**V**, **X**, **Y**, **Z**). A brief description of each period is summarized in Table S1. In period **V**, the electronic zero of the H_2O_2 analyzer ($[H_2O_2]_0$) was measured while water vapor diffused into the lipid coating. The reactant ozone ($[O_3]_0$) was measured in period **X**, where the reactor bypass line was directly connected to the analyzers. Using the two three-way valves, air was directed to the reactor to initiate the lipid ozonolysis reaction (period **Y**). During this period, the instantaneous H_2O_2 mixing ratio at any given timepoint *t* ($[H_2O_2]_t$) was calculated through eq. S1.

$$[\mathrm{H_2O_2}]_t = [\mathrm{H_2O_2}]_{\mathrm{reaction}} - [\mathrm{H_2O_2}]_0 \quad \text{(eq. S1)}$$

where $[H_2O_2]_{reaction}$ was the instantaneous reading from the H_2O_2 analyzer at *t*. After the reaction period **Y**, the reactant air was re-measured in the bypass line ($[O_3]_{end}$) to observe any change in the ozone supply as the reaction was proceeding (typically < 10 ppb after more than 6 hours of 500 ppb ozone generation, period **Z**). With all ozone measurements above, the instantaneous O_3 consumption by the lipid at any given point *t* ($\Delta[O_3]_t$) during the reaction was calculated through eq. S2.

$$\Delta[\mathrm{O_3}]_t = [\mathrm{O_3}]_0 - [\mathrm{O_3}]_{\mathrm{reaction}} - [\mathrm{O_3}]_{\mathrm{wall}} - \frac{n}{N}([\mathrm{O_3}]_0 - [\mathrm{O_3}]_{\mathrm{end}}) \quad \text{(eq. S2)}$$

where $[O_3]_{reaction}$ was the instantaneous reading from the ozone monitor at *t*, *n* was the *n*th (integer) hour in which *t* situates in period **Y** and *N* was the total length (hr) of the reaction period **Y**.

The H_2O_2 yield from the reaction was calculated through the ratio of H_2O_2 formation to ozone consumption by the lipid (eq. S3). For hourly yields, the average $[H_2O_2]$ and average $\Delta[O_3]$ were taken every 60 minutes in period **Y** and the uncertainty was calculated through the propagation of one standard deviation (1σ) uncertainties of hourly $[H_2O_2]$ and $\Delta[O_3]$. The calculated $[H_2O_2]$, $\Delta[O_3]$ and hourly H_2O_2 yields during the first six hours in period **Y** of Figure S2 are shown in Figure 3a. Finally, the overall yield of the reaction was calculated through the average of all hourly yields up to 16 hours, with the exclusion of the first hour due to high signal variation during this time. The uncertainty is reported as the 1σ confidence interval of the hourly yields.

$$H_2O_2 \text{ yield} = \frac{\overline{[\mathrm{H_2O_2}]}}{\overline{\Delta[\mathrm{O_3}]}} \quad \text{(eq. S3)}$$

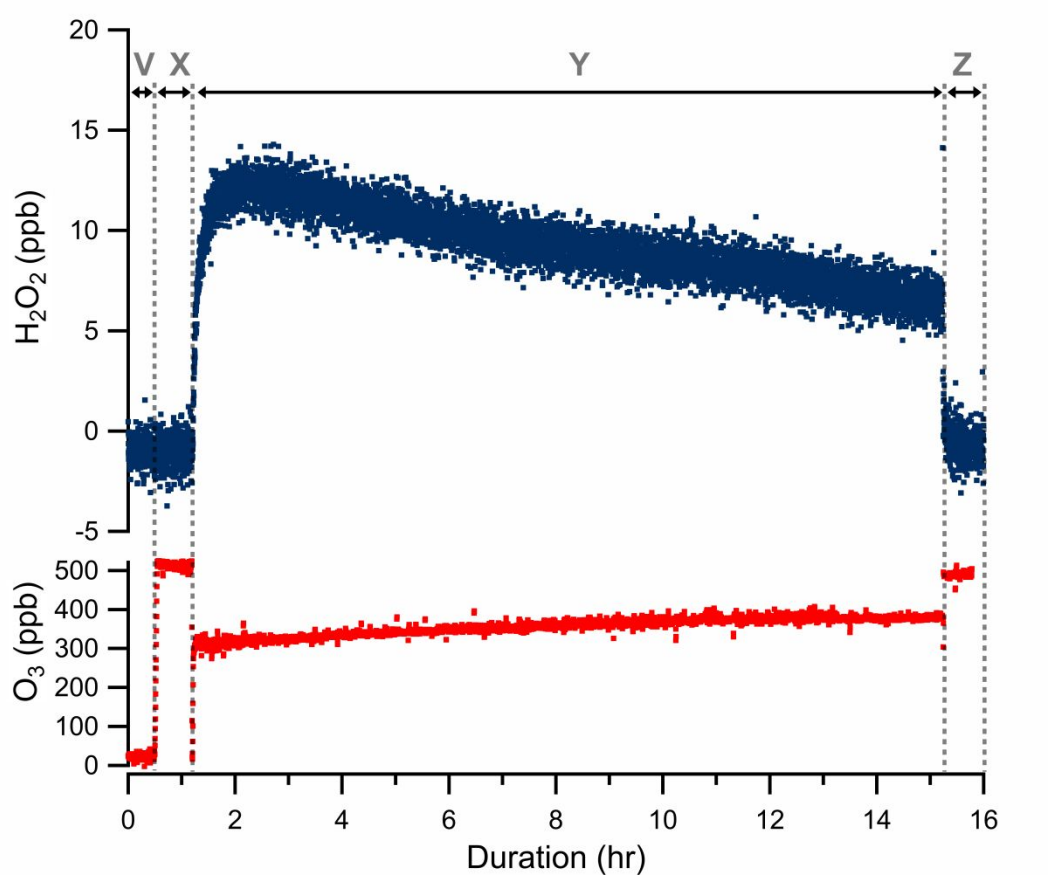

Figure S2. Representative four-period measurements of H_2O_2 and O_3 during the oxidation of 7.5 µL triolein under 500 ppb O_3 and 50% RH.

Table S1. Description and purpose of each time period during quantitation measurements.

Time period	Process Description	Purpose
V (~ 30 mins)	Humidified zero air passing through the flow tube reactor containing coated lipid	Equilibrating lipid with water vapor and measurement of the electronic zero of the H_2O_2 analyzer ($[H_2O_2]_0$)
X (~ 30 mins)	Directing air to the reactor bypass line with the addition of O_3 (reactant air)	Measurement of the reactant O_3 ($[O_3]_0$)
Y (6 – 16 hrs)	Directing reactant air to the reactor (initiation of ozonolysis reaction)	Measurement of O_3 ($[O_3]_{reaction}$) and H_2O_2 ($[H_2O_2]_{reaction}$) inside the reactor at any given point during the reaction
Z (~ 30 mins)	Directing reactant air to the reactor bypass line after the reaction	Post-reaction measurement of the reactant O_3 ($[O_3]_{end}$)

3) Ozonolysis mechanism

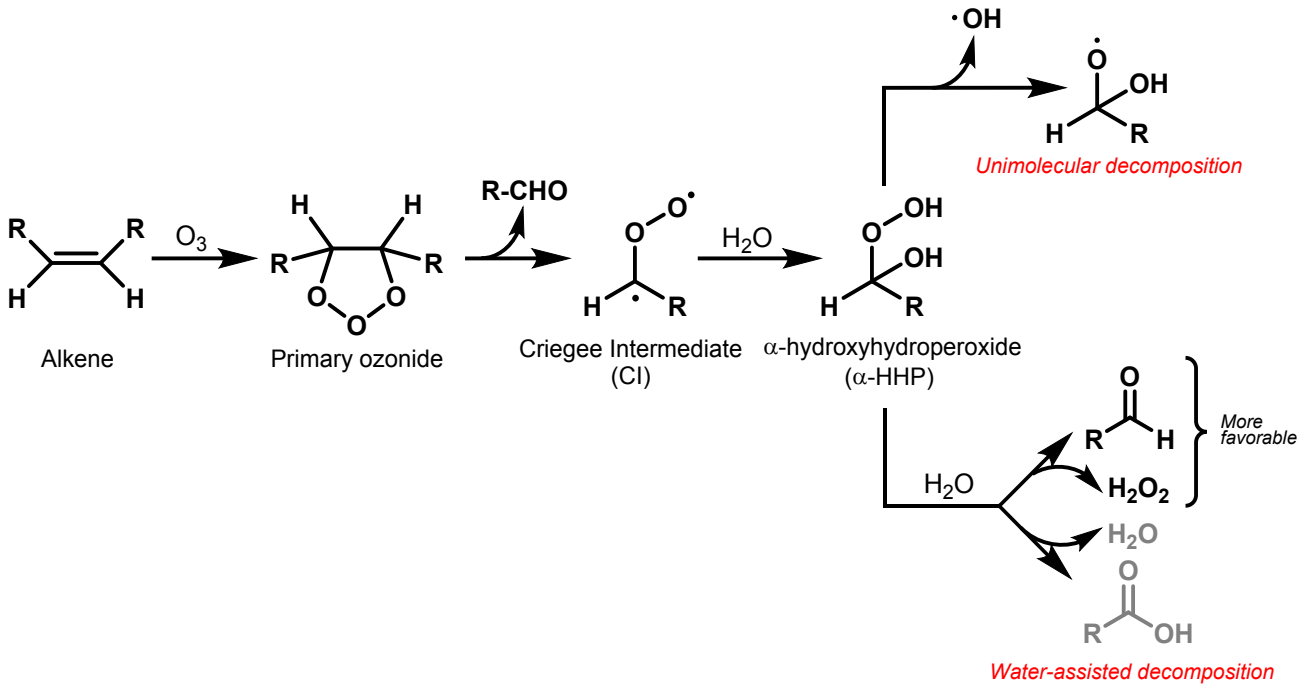

Figure S3. Possible degradation pathways for α-hydroxyhydroperoxide (α-HHP) in the gas phase.

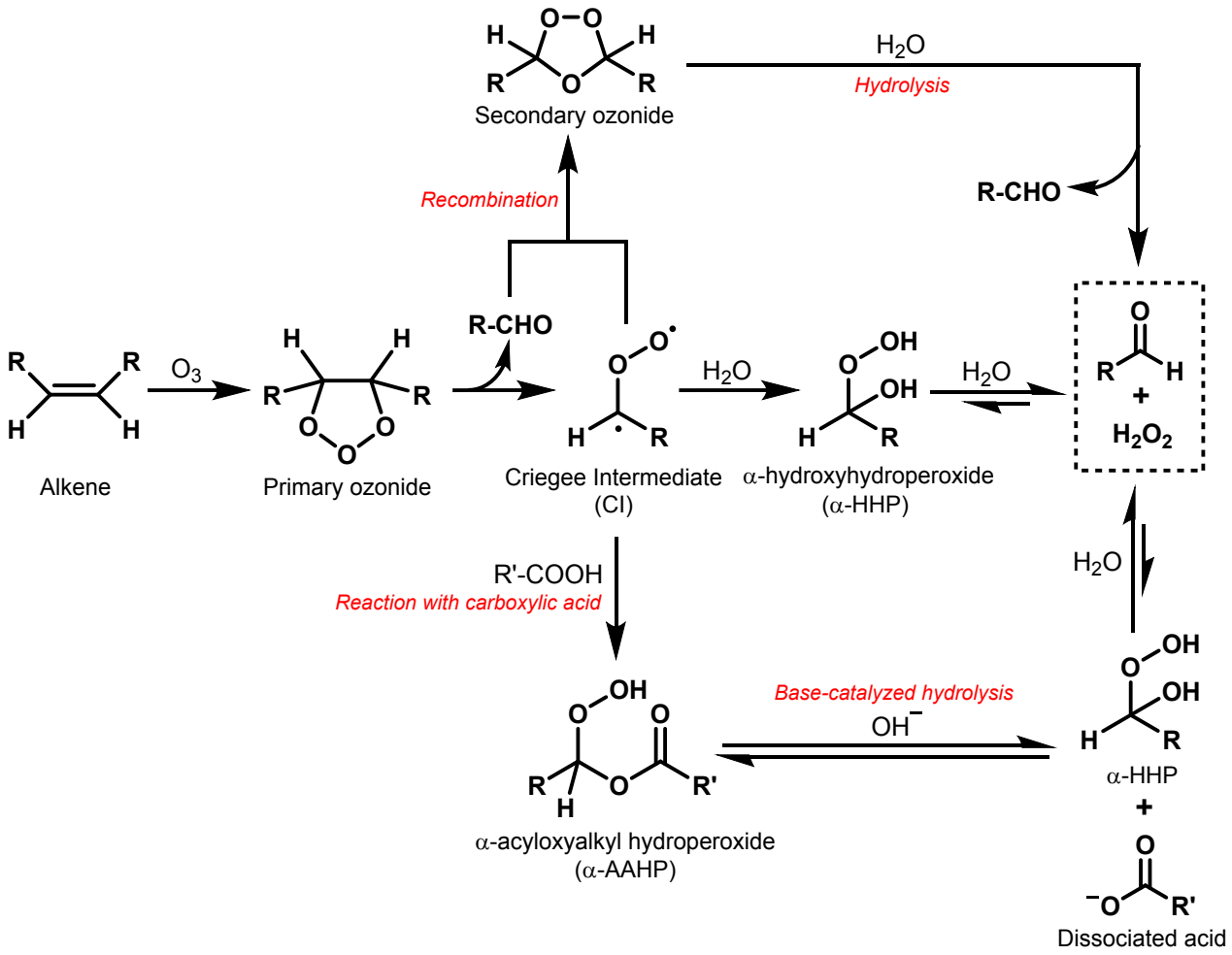

Figure S4. Competitive reactive pathways of Criegee Intermediate and relevant H_2O_2 formation mechanisms in the aqueous phase.

4) Lifetimes of hydroxyhydroperoxides (α-HHPs) derived from oxidized methyl oleate

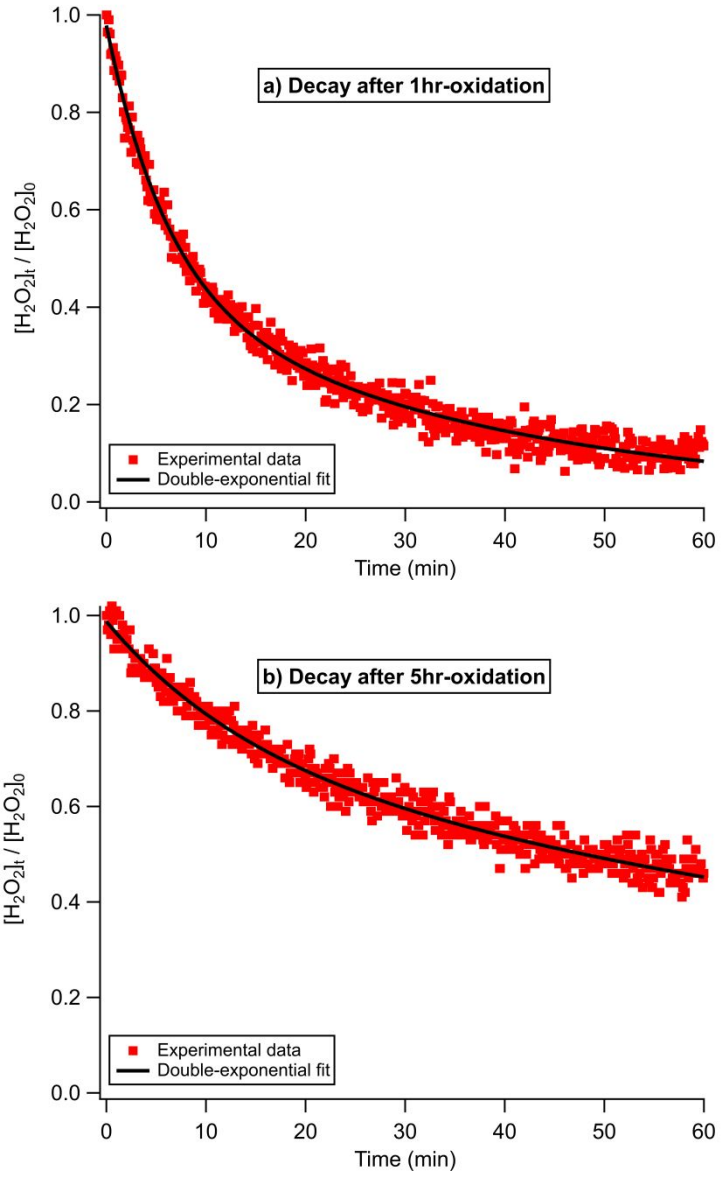

Figure S5. Relative H_2O_2 signal decay, along with its double-exponential fit, measured immediately after about **a)** 1-hour and **b)** 5-hour oxidation of 7.5 µL coated methyl oleate (500 ppb ozone, ≥50% RH). During the decay, RH was kept at 50% and no ozone was generated. Note that **a)** was derived from **D** ➔ **E** in Figure 2a.

In the H_2O_2 decay periods under elevated RH and zero ozone demonstrated in Figure 2, the lifetime of α-HHPs can be calculated from the e-folding time derived from the H_2O_2 signal decay. Such applicable periods include **D** ➔ **E** (also shown in Figure S5a), **G** ➔ **end** and **L** ➔ **M**. In

addition, the decay signal after 5-hour oxidation of methyl oleate coating under high RH is shown in Figure S5b (not a part of Figure 2). The H_2O_2 mixing ratio recorded immediately after the partial oxidation of the lipid under high RH is set as $[H_2O_2]_0$ (at t = 0) to which the subsequent H_2O_2 measurements are normalized. For a single-exponential lifetime (τ), the decay profile is fitted through eq. S4. For the best result, *A* was held between 0.9 and 1 to accommodate the long timescale offset *b*, which varies between 0 and 0.1.

$$\frac{[H_2O_2]_t}{[H_2O_2]_0} = Ae^{-\frac{t}{\tau}} + b \quad \text{(eq. S4)}$$

Since the release of H_2O_2 may involve both chemical decomposition and mass transfer processes of water, ozone and H_2O_2, the decay plot was better fit with more parameters, as with a double-exponential function shown in eq. S5. The offset *b* was held to 0. Two lifetimes, τ_1 and τ_2, are derived to demonstrate the slow and fast components of the kinetics. Figure S5 shows the examples of this fitting and Table S2 summarizes the single- and double-exponential lifetimes derived for α-HHPs.

$$\frac{[H_2O_2]_t}{[H_2O_2]_0} = A_1e^{-\frac{t}{\tau_1}} + A_2e^{-\frac{t}{\tau_2}} + b \quad \text{(eq. S5)}$$

Table S2. Single- and double-exponential lifetimes of methyl oleate based α-HHPs at different stages of reaction.

Decay period	Single-exponential lifetime (τ, min)	Double-exponential lifetimes	
		τ_1 (min)	τ_2 (min)
D ➔ E in Figure 2a (also Figure S5a or 1 hour after oxidation)	10	36	6
G ➔ end in Figure 2a	2	23	2
L ➔ M in Figure 2b	2	18	2
Figure S5b (i.e. after 5 hours of oxidation)	76	135	15

5) Box model analysis of indoor H_2O_2 formation

We estimate an upper limit of the H_2O_2 mixing ratio in an indoor environment based on the measurements in this study. In particular, we assume that indoor ozone is lost via reaction with double bonds in molecules on surfaces (assuming O_3 mixing ratio = 5 ppb)[2] with a typical deposition velocity (v_D) of 0.04 cm s^{-1}.[3] Based on an intermediate value of the yields measured in this work, the molar yield of H_2O_2 with respect to ozone consumption ($Y_{H_2O_2}$) is assumed to be 0.1. We do the calculation for an indoor space with surface area to volume (*S/V*) ratio of 3 m^{-1}.[4] We then equate this production rate to the loss rate of H_2O_2 assuming steady state for an indoor volume that has an air exchange rate (*AER*) of 1 hr^{-1}.[5]

This calculation based on eq. S6 predicts a H_2O_2 mixing ratio of 2 ppb under steady state. This is an upper limit to the indoor gas phase H_2O_2 for two reasons. One, some ozone may be lost on indoor surfaces via reactions that do not lead to H_2O_2. Two, as with most molecules, H_2O_2 will reside largely on indoor surfaces existing in a dynamic equilibrium with smaller amounts in the gas phase.[6]

$$\frac{d[H_2O_2]}{dt} = 0 = v_D\,[O_3]\,Y_{H_2O_2}\left(\frac{S}{V}\right) - [H_2O_2]\,AER \quad \text{(eq. S6)}$$

References

[1] Kahan, T. F.; Washenfelder, R. A.; Vaida, V.; Brown, S. S. Cavity-Enhanced Measurements of Hydrogen Peroxide Absorption Cross Sections from 353 to 410 nm. *J. Phys. Chem. A* **2012***, 116*, 5941-5947.

[2] Deming, B. L.; Ziemann, P. J. Quantification of alkenes on indoor surfaces and implications for chemical sources and sinks. *Indoor Air* **2020***, 30*, 914-924.

[3] Nazaroff, W. W.; Gadgil, A. J.; Weschler, C. J. Critique of the use of deposition velocity in modeling indoor air quality. In *Modeling of indoor air quality and exposure,* Nagda, N. L., Ed.; American Society for Testing and Materials: Philadelphia, 1993; Vol. ASTM STP 1205, pp 81–104.

[4] Manuja, A.; Ritchie, J.; Buch, K.; Wu, Y.; A. Eichler, C. M.; C. Little, J.; C. Marr, L. Total surface area in indoor environments. *Environ. Sci.: Processes & Impacts* **2019***, 21*, 1384-1392.

[5] Abbatt, J. P. D.; Wang, C. The atmospheric chemistry of indoor environments. *Environ. Sci.: Processes Impacts* **2020***, 22*, 25-48.

[6] Wang, C.; Collins, D. B.; Arata, C.; Goldstein, A. H.; Mattila, J. M.; Farmer, D. K.; Ampollini, L.; DeCarlo, P. F.; Novoselac, A.; Vance, M. E. Surface reservoirs dominate dynamic gas-surface partitioning of many indoor air constituents. *Sci. adv.* **2020***, 6*, eaay8973.